

1
2
3 The anaerobic rheological behaviour of digested sludge
4

5 J.C. Baudez^{1,2}, F. Markis², N., Eshtiaghi², P. Slatter²
6

7 1 Cemagref, UR TSCF, F-03150 Montoldre, France

8 2 Rheology and Materials Processing Centre, Dept. of Chemical Engineering, RMIT University,
9 Victoria, Australia, 3001
10

11
12 Corresponding author: jean-christophe.baudez@cemagref.fr
13

14 Abstract
15

16 Producing biogas energy from the anaerobic digestion of wastewater sludge is one of the most
17 challenging tasks facing engineers, because they are dealing with vast quantities of fundamentally
18 scientifically poorly understood and unpredictable materials; while digesters need constant flow
19 properties to operate efficiently. An accurate estimate of sludge rheological properties is required
20 for the design and efficient operation of digestion, including mixing and pumping. In this paper, we
21 have determined the rheological behaviour of digested sludge at different concentrations, and
22 highlighted common features. At low shear stress, digested sludge behaves as a linear viscoelastic
23 solid, but shear banding can occur and modify the apparent behaviour. At very high shear stress,
24 the behaviour fits well to the Bingham model. Finally, we show that the rheological behaviour of
25 digested sludge is qualitatively the same at different solids concentrations, and depends only on
26 the yield stress and Bingham viscosity, both parameters being closely linked to the solids
27 concentration.
28

29 Keywords
30

31 Digested sludge, Bingham model, Herschel-Bulkley model, shear banding, viscoelasticity.
32

33 Introduction
34

35 Renewable energy is said to be one of the pillars of sustainable management. Biogas from the
36 anaerobic digestion of sewage sludge can provide a clean, easily controlled source of renewable
37 energy from sewage sludge, replacing fossil fuels. However, an accurate estimate of sludge
38 rheological properties is required for the design and efficient operation of the pumping systems
39 which surround anaerobic digesters (Slatter, 1997, 2003). Indeed Tarp and Melbinger (1967)
40 showed the significant advantages of recycling and recirculating digested sludge to mix it with

41 excess sludge, among them an increase in biogas production (Sperry, 1959). The mixture can be
42 concentrated to a much higher solid content than would be possible for the excess sludge alone,
43 and recirculation also facilitates improved mixing efficiency over mechanical stirring. However, the
44 flow rate in the recirculation circuits has to be very large (Appels et al, 2008) and rheology is
45 needed to calculate head losses and pumping power (Slatter, 2001).

46 Except for the work of Monteiro (1997) who showed that anaerobic digestion induces a decrease of
47 the rheological characteristics of sludge, most investigations on sludge rheology were focused on
48 activated sludge. No reliable data, at high shear rate (within recirculation pipes), can be found in
49 the literature for digested sludge while at low shear rate (within the digester), results are scarce
50 and not always usable. Most of these were obtained by applying shear rate ramps that gave
51 distinct peaks in the flow curve (for example, Ayol et al., 2005), but Baudez (2006) clearly
52 established that these peaks in the flow curves were principally instrument artefacts, and not
53 material characteristics. However, the work of Ayol et al. (2005) pointed out that with very dilute
54 sludge, the Ostwald model, i.e. a power law model with no yield stress, gave the best fit.

55 From a physical perspective, digested sludge appears to be a stable suspension with low settling
56 rates (Namer and Ganczarczyk, 1993) and low surface charge (Forster, 2002), implying that
57 interactions are more steric than electrostatic. The most important constituents in digested sludge
58 are lipopolysaccharides (Forster, 1983) which are amphiphile lipids with both hydrophilic and
59 hydrophobic heads. These molecules displayed a very intriguing rheological behaviour (Muñoz et
60 al, 2000), showing linear viscoelasticity, non-Newtonian viscous flow and shear banding (Miller and
61 Rothstein, 2007).

62 In this paper, our intention is to establish the basic characteristics of the rheological behaviour of
63 digested sludge, with the objective of industrial applications in digester mixing, pumping and pipe
64 flows, meaning that we will focus on short-term behaviour. Short-term behaviour means we will not
65 focus our research on eventual thixotropic effects. As predicted by the literature on amphiphile
66 rheology, we show that digested sludge exhibits linear viscoelastic behaviour at low shear
67 stresses, followed by shear-banding phenomena at intermediate stresses, and finally a non-
68 Newtonian fluid behaviour with a yield stress, modelled by a Herschel-Bulkley model at
69 intermediate shear rates and by a Bingham model at very high shear rates. We also highlight the
70 fact that the rheological behaviour is qualitatively the same at different solid concentrations,
71 allowing us to define a master-curve for which the dimensionless parameters are the yield stress
72 and the Bingham viscosity.

73

74 Material and methods

75

76 The digested sludge was sampled at the Mount Martha waste water treatment plant (Melbourne,
77 Victoria, Australia) at the outlet of the digester number 1. Its initial solid concentration was at
78 18.5g.L^{-1} and was also gently concentrated to 25.5, 32 and 49g.L^{-1} by using a Buchner vacuum.
79 Sludge samples were stored at 4°C for 30 days before experiments, in order to reduce temporal
80 variability. Indeed, even after anaerobic digestion, sludge may not be fully stabilised and organic

81 changes may still occur. By storing the sludge sample for such an extended period, the potential
82 for composition changes is reduced; and we can assume that we used exactly the same material
83 throughout all our experiments.

84

85 Rheological measurements were performed with a DSR200 instrument from Rheometric Scientific,
86 connected to a temperature controlled water bath. The rheometer was equipped with a cup and
87 bob geometry (inner diameter: 29mm, outer diameter: 32mm, length: 44mm). Temperature was
88 kept at 25°C. To avoid evaporation, sludge was covered with a thin film of immiscible Newtonian
89 oil.

90 Before each measurement, sludge was presheared for 10 minutes at a shear rate of 1000s⁻¹ then
91 left at rest for 10 minutes. This procedure allowed us to erase material memory and to have
92 reproducible measurements. Then, different tests were performed:

- 93 • Shear stress sweep, by applying a linear ramp of increasing stress over time. In this test,
94 we changed the time of rest between preshear and shear, from 1 to 60 minutes in order to
95 investigate structural changes occurring during rest;
- 96 • Creep test, by applying constant shear stress and measuring the corresponding shear
97 strain, at different shear stresses in the linear viscoelastic regime and above;
- 98 • Decreasing stress ramp to determine the flow curve, starting at a high stress corresponding
99 to a shear rate of approximately 1000s⁻¹ or lower for the less concentrated sludge (to avoid
100 turbulent conditions).

101

102

103 Results and discussion

104

105 Starting from rest, the shear stress sweep first elicits a linear viscoelastic response from the
106 digested sludge up to a critical shear stress τ_0 above which the material apparently starts to flow
107 (Fig. 1). In the linear viscoelastic region, the behaviour is modelled by a generalised Kelvin-Voigt
108 model, with a wide relaxation time spectrum modelled by a stretched exponential:

$$109 \quad \gamma(t) = \tau \cdot \frac{1}{G} \cdot \left(1 - \exp(-(\lambda t)^m)\right) \quad (1)$$

110 where γ represents the strain, τ the stress and $\lambda = \frac{G}{\mu}$ with G and μ the usual parameters of a

111 Kelvin-Voigt model.

112 Assuming that the sludge is flowing in its liquid regime above the critical shear stress following a
113 Herschel-Bulkley model (Monteiro, 1997), the additional strain can be expressed as:

$$114 \quad \gamma(t) = \int_{t_0}^t \dot{\gamma} du = \int_{t_0}^t \left(\frac{\tau - \tau_0}{K}\right)^{1/n} = \int_{t_0}^t \left(\frac{a \cdot x - a \cdot t_0}{K}\right)^{1/n} dx = \frac{a \cdot n}{(n+1)K} (t - t_0)^{1+1/n} \quad (2)$$

115 where a is the slope of the shear stress ramp and t_0 the time such that the shear stress equals the
116 yield stress of the Herschel-Bulkley model $\tau_0 = a \cdot t_0$.

117 Thus, the total strain, which predicts the experimental data (Fig. 1), can be expressed as:

$$118 \quad \gamma(t) = \tau \cdot \frac{1}{G} \cdot \left(1 - \exp(-(\lambda t)^n)\right) + b \cdot (t - t_0)^{1+1/n} \quad (3)$$

$$119 \quad \text{with } b = \frac{an}{(n+1) \cdot K}$$

120 Applying this to the experimental data gave a flow behaviour index for the Herschel-Bulkley model,
121 n , greater than 1 (Fig. 1), meaning that the digested sludge could apparently be a shear-thickening
122 liquid above τ_0 , which is unusual.

123 Creep tests confirmed a change in the behaviour above τ_0 . Below τ_0 , the strain slowly increased
124 with time, while above τ_0 , the increase is faster (Fig. 2), both following a power law with time.

125 However, even for stresses higher than τ_0 (Fig. 2) the shear strain follows a power-law with a
126 power-law index less than 1, indicating that the shear rate is a decreasing function of time: there is
127 no steady state and so, sludge is restructuring and not flowing (otherwise, the shear rate would
128 have been constant over time for a constant shear stress). The value τ_0 cannot therefore be
129 considered as a classical yield stress above which digested sludge flows in its liquid regime. These
130 power-law relationships between strain and time are in fact a consequence of a structural
131 relaxation process which occurs during creep (Baudez, 2008).

132 When the time of rest between the preshear and the stress sweep increases, the behaviour is
133 globally the same, with first a linear viscoelastic behaviour (Fig. 3) but the critical shear stress, τ_0
134 decreases with increase of the time of rest, the global elasticity decreases, the mean relaxation
135 time (inverse of λ) increases and the strain corresponding to τ_0 decreases (Fig. 4): the longer the
136 time of rest, the smaller the linear viscoelastic range.

137 At rest, the digested sludge structure became weaker and weaker (decrease of τ_0 and elasticity)
138 but concurrently the relaxation time increased, indicating an evolution from a viscoelastic material
139 towards a more elastic solid (the decrease of μ is faster than the decrease of G). Since this is
140 physically impossible, this observed apparent behaviour is not representative of the true material
141 behaviour but derives from erroneous interpretation of raw data.

142 Above τ_0 , experimental results showed the viscosity is globally decreasing, which is inconsistent
143 with the apparent shear-thickening behaviour noted earlier, but oscillations of viscosity regarding
144 shear stress are reported (Fig. 5). These oscillations indicated local minima in the flow curve where
145 apparent shear rate occasionally decreased while shear stress increased.

146 If we assume the relationship between local shear rate and local shear stress is monotonic, then
147 we can write:

$$148 \quad \dot{\gamma} = f(\tau) \text{ where } f \text{ is the inverse function of the behaviour law.}$$

149 In a Couette geometry, the shear rate can be expressed as:

$$150 \quad \dot{\gamma}_{local} = -r \cdot \frac{\partial(\omega)}{\partial r} \Leftrightarrow \omega = \int_{R_1}^{R_2} \frac{\dot{\gamma}_{local}}{r} dr \Leftrightarrow \omega = \int_{R_1}^R \frac{f(\tau_{local})}{r} dr \quad (4)$$

151 where ω is the angular velocity, R_1 the inner radius and $R - R_1$ the thickness of the sheared
152 region. The maximum value of $R - R_1$ is $R_2 - R_1$, where R_2 is the outer radius.

153 The apparent shear rate is calculated from the measured angular velocity, the only raw data
154 measured by the rheometer. The shear rate given by the rheometer is calculated with the
155 assumption of a full shear within the gap. So, if the apparent shear rate decreased, it means the
156 angular velocity decreased. However, because f is a monotonic function, this decrease of ω is
157 rather the consequence of a decrease of the effective gap $R - R_1$, implying that shear banding has
158 occurred during the measurement.

159 Such behaviour (shear banding and viscoelastic behaviour) has to be taken into account in
160 digester design and operation, because shear banding means that there is coexistence of both
161 sheared and unsheared zones in the digester, these last being useless, unmixed, dead zones.

162 According to Moller et al. (2008), the width of the flowing band can be directly related to the
163 macroscopically imposed shear rate. At high shear rates, the whole gap is sheared and when the
164 applied stress is much higher than τ_0 , the sludge flows normally, with no apparent perturbation
165 effects, allowing us to have achieved reproducible measurements (Fig. 6) with the corresponding
166 smooth classical shape of the flow curve.

167 As expected, the higher the concentration, the thicker the sludge (Fig. 7) but depending on the
168 shear rate range, different well-known models can be used to describe the rheological behaviour of
169 digested sludge. At high shear rates, a basic Bingham model is sufficient (Fig. 8) while at low and
170 intermediate shear rates, Herschel-Bulkley and power-law models are more appropriate (Fig 9).
171 They all represent the same material but can only be used in a specific range of validity, regarding
172 the complexity of the process to be modelled. Thus, for pumping where shear rates are very high,
173 a Bingham model would be appropriate since it deals with simple characteristics, i.e. a yield stress
174 and a constant rheogram slope above it.

175 From a more general point of view, in the liquid regime we can summarize the rheological
176 behaviour of digested sludge as a shear-thinning yield stress fluid with a plateau viscosity at high
177 shear rates:

$$178 \quad \tau = \tau_c + \eta(\dot{\gamma}) \cdot \dot{\gamma} \text{ with } \eta(\dot{\gamma}) \xrightarrow{\dot{\gamma} \rightarrow \infty} \alpha_0$$

179 Moreover, at low and intermediate shear stresses, $\tau = \tau_c + K \cdot \dot{\gamma}^n = \tau_c + \eta(\dot{\gamma}) \cdot \dot{\gamma} \Leftrightarrow \eta(\dot{\gamma}) \approx K \cdot \dot{\gamma}^{n-1}$

180 Thus, for the sake of simplicity, we define the rheological behaviour of digested sludge as follows:

$$181 \quad \tau = \tau_c + \left(K \cdot \dot{\gamma}^{n-1} + \alpha_0 \right) \cdot \dot{\gamma} \quad (5)$$

182 On our range of data, i.e. below $1000s^{-1}$, this model was successful. However, if $\dot{\gamma} \ll \sqrt[n-1]{\frac{K}{\alpha_0}}$, the

183 Herschel-Bulkley model is sufficient to model the behaviour, which corresponds to a shear rate

184 smaller than 565s^{-1} for the most concentrated sludge and smaller than 145 s^{-1} for the less
 185 concentrated sludge as shown below (Table 1).

186

187

Table 1: Shear rate above which the Herschel-Bulkley model is not suitable

Concentration [%]	Limit shear rate [s-1]
1.85	145
2.56	280
3.17	470
4.89	565

188

189 Equation (5) can also be expressed as:

$$\tau = \tau_c + K \cdot \dot{\gamma}^n + \alpha_0 \cdot \dot{\gamma}$$

$$\Leftrightarrow \frac{\tau}{\tau_c} = 1 + \frac{K}{\tau_c} \cdot \dot{\gamma}^n + \frac{\alpha_0}{\tau_c} \cdot \dot{\gamma}$$

190

$$\Leftrightarrow \frac{\tau}{\tau_c} = 1 + \beta \cdot \Gamma^n + \Gamma \tag{6}$$

$$\Gamma = \frac{\alpha_0}{\tau_c} \cdot \dot{\gamma}, \beta = \frac{K}{\tau_c} \cdot \left(\frac{\tau_c}{\alpha_0} \right)^n$$

191

192 In such a dimensionless form, all the flow curves are similar, independent of solids concentration
 193 (Fig. 10). From a physical point of view, this result means that there is some similarity of the
 194 network of interactions within the sludge at different concentrations, which is at the origin of the
 195 similarity of its macroscopic behaviour. In such suspensions, interactions can be classified into two
 196 main groups (Baudez and Coussot, 2001): hydrodynamic interactions (between solid particles and
 197 surrounding fluid, here basically represented by the Bingham viscosity) and non-hydrodynamic
 198 interactions (between solid particles, basically represented by the yield stress). Increasing the
 199 concentration doesn't change the nature of these interactions, but rather modifies their relative
 200 intensity. The dimensionless form smoothed these differences because both kinds of interactions
 201 in this form will approach unity.

202 On our range of concentrations, yield stress and Bingham viscosity increase with the solid
 203 concentration (Fig. 11) respectively following a power-law and an exponential law of the following
 204 form, which is in agreement with the literature, both for the yield stress (Baudez, 2008) and the
 205 Bingham viscosity (Sanin, 2002):

$$\tau_c = \alpha \cdot (\phi - \phi_0)^m \tag{7}$$

$$k_2 = \mu_0 \cdot \exp(\beta \cdot \phi) \tag{8}$$

208 where ϕ_0 is the lowest concentration below which there is no yield stress, m is related to the fractal
 209 dimension of sludge flocs (Baudez, 2008) and μ_0 is the viscosity of the liquid medium.

210 We found that the value μ_0 is twice that of pure water, which can be explained by the large
211 amount of dissolved matter present, which may increase the supernatant viscosity.

212

213

214 Conclusion

215

216 In this paper, we have shown that digested sludge is a shear-thinning yield stress fluid, presenting
217 flow instabilities at low shear rates, manifesting as shear banding. At low shear stress, below the
218 yield stress, digested sludge behaved as a viscoelastic solid. When the applied stress is increased,
219 above a critical shear strain, which decreases with the restructuring, shear banding appears. Then,
220 at higher stresses, digested sludge behaves like a yield stress fluid and can be modelled using
221 both the Herschel-Bulkley and Bingham plastic models over a wide range of shear rates.

222 This behaviour was similar at different concentrations and yield stress followed a power-law with
223 the concentration while the Bingham viscosity followed an exponential law with concentration.

224 By reducing the rheological parameters with the yield stress and the Bingham viscosity, which
225 have to be measured separately, a master curve was obtained. This result means that the
226 rheological behaviour of the digested sludge at any concentration can be deduced from this master
227 curve.

228 However, further work has to be done on shear banding. This behaviour will have to be taken into
229 account in digester design and process operations, in order to avoid dead zones in the digester.

230

231 Acknowledgements

232

233 The authors acknowledge the Cemagref-RMIT agreement for our collaboration

234

235 References

236

237 Appels, L., Baeyens, J., Degève, J., Dewil, R., 2008. Principles and potential of the anaerobic
238 digestion of waste-activated sludge. Progress in Energy and Combustion Science Volume 34,
239 Issue 6, December 2008, Pages 755-781

240 Ayol, A., Filibeli, A., Dentel, S.K., 2006. Evaluation of conditioning responses of thermophilic-
241 mesophilic anaerobically and mesophilic aerobically digested biosolids using rheological
242 properties. Water Science and Technology, 54, 5, 23-31.

243 Baudez, J.C., Coussot, P., 2001. Rheology of aging, concentrated, polymeric suspensions -
244 Application to pasty sewage sludges. J. Rheol. 45(5):1123-1139.

245 Baudez, J.C., 2006. About peak and loop in sludge rheogram. Journal of Environmental
246 Management, 78, 232-239.

247 Baudez, J.C., 2008. Physical aging and thixotropy in sludge rheology. Applied Rheology, 18,
248 13495 1-8.

249 Forster, C.F., 1983. Bound water in sewage sludge and its relationship to sludge surfaces and
250 sludge viscosities. *J. Chem. Tech. Biol.*, 33B:76-84.

251 Forster, C.F., 2002. The rheological and physico-chemical characteristics of sewage sludge".
252 *Enzyme and Microb. Tech.*, 30(3):340-345.

253 Miller, E., Rothstein, J.P., 2007. Transient evolution of shear banding in wormlike micelle solutions.
254 *J. Non-Newtonian Fluid Mech.* 143, 22–37

255 Moller, P. C. F, Rodts, S. Michels, M. A. J. and Bonn, D., 2008. Shear banding and yield stress in
256 soft glassy materials. *Phys. Rev. E* 77, 041507.

257 Monteiro, P.S., 1997. The influence of the anaerobic digestion process on the sewage sludges
258 rheological behaviour. *Wat. Sci. Tech.*, 36 (11): 61-67

259 Munoz, J., Alfaro, M.C., 2000. Rheological and phase behaviour of amphiphilic lipids. *Grasas y*
260 *aceites*, vol. 51, pp. 6-25

261 Namer, J. J. Ganczarczyk, L., 1993. Settling Properties of Digested Sludge Particle Aggregates.
262 *Water Research*, 27, 1285-1294

263 Sanin, F.D., 2002. Effect of solution physical chemistry on the rheological properties of activated
264 sludge. *Water SA*, 28: 207-212.

265 Slatter P. 1997. The rheological characterisation of sludges. *Wat. Sci. Tech.* 36(11), 9-18.

266 Slatter P. 2001. Sludge pipeline design, *J. Wat. Sci. Tech.* 44(10):115-120.

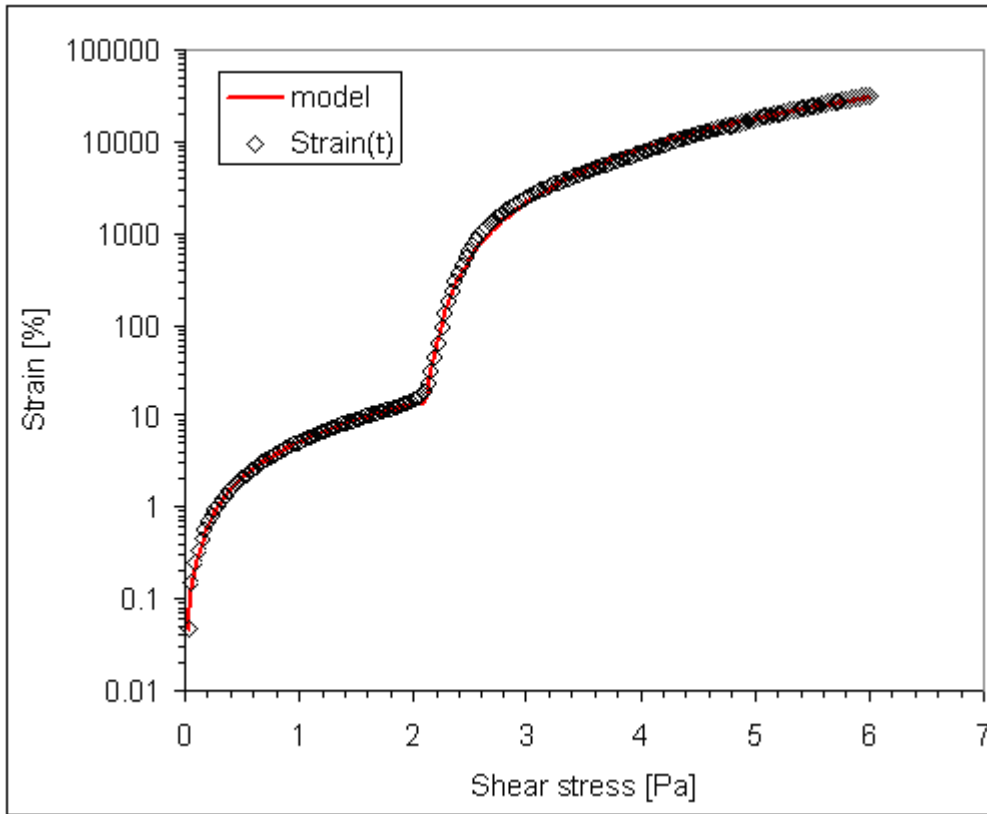
267 Slatter P. 2003. Pipeline transport of thickened sludges. *Water* 21: 56-57.

268 Tropey, W. N. and Melbinger, N. R., 1967. Reduction of Digested Sludge Volume by Controlled
269 Recirculation. *Journal Water Pollution Control Federation* 39(9): 1464-1474.

270 Sperry, W.A., 1959. Gas Recirculation at Aurora, Illinois, *Sewage and Industrial Wastes* vol. 31, n
271 6.

272 Captions

273



274

275

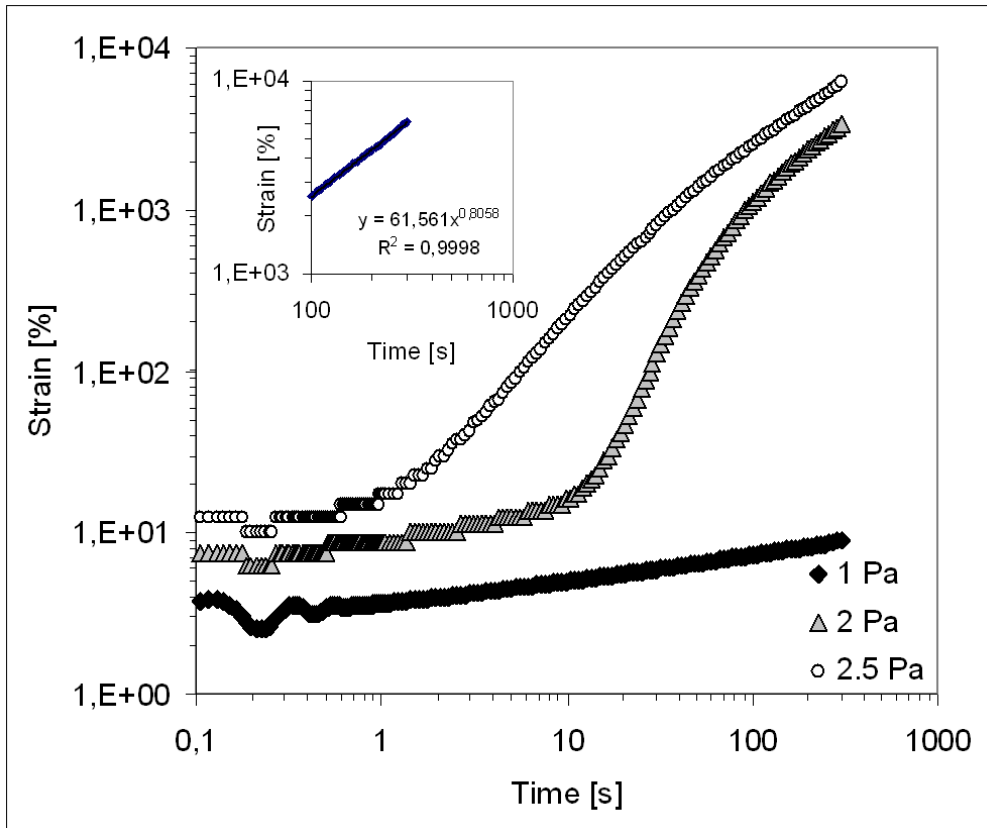
276

277

278

279

Figure 1: Strain-stress behaviour of the 4.9% digested sludge. The dashed lined corresponds to the model of (1) with $G=0.62\text{Pa}$, $\lambda=3.3\cdot 10^{-7}\text{s}^{-1}$, $m=0.34$, $b=0.35\text{s}^{-2}$, $t_0=315.5\text{s}$, corresponding to a stress equals to 2.13Pa and $n=1.30$.



280

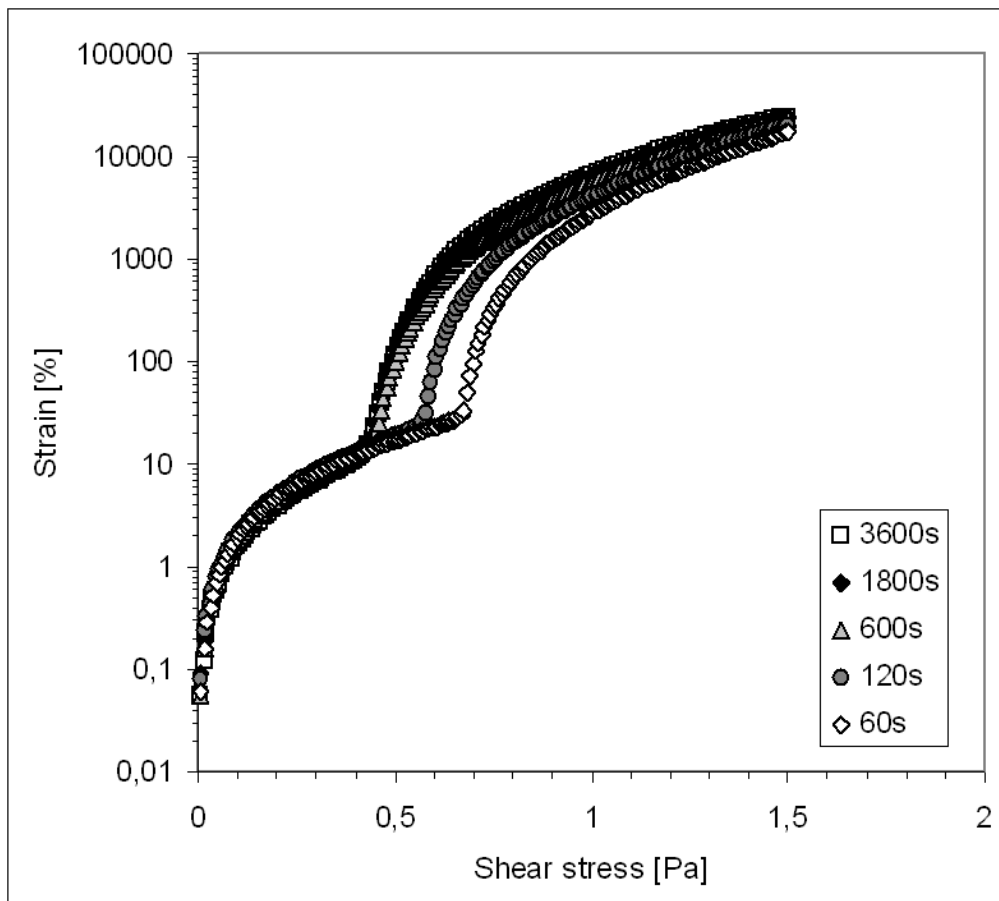
281

Figure 2: Creep test below, above and equal to the critical shear stress. Here, the critical stress is 2.5 Pa for the 4,9% sludge. The insert is a focus on the strain at the highest strain at longer time, following a power-law with an index smaller than 1.

282

283

284



285

286

Figure 3: strain stress behaviour when a stress sweep is applied after different time of rest.

287
288
289
290

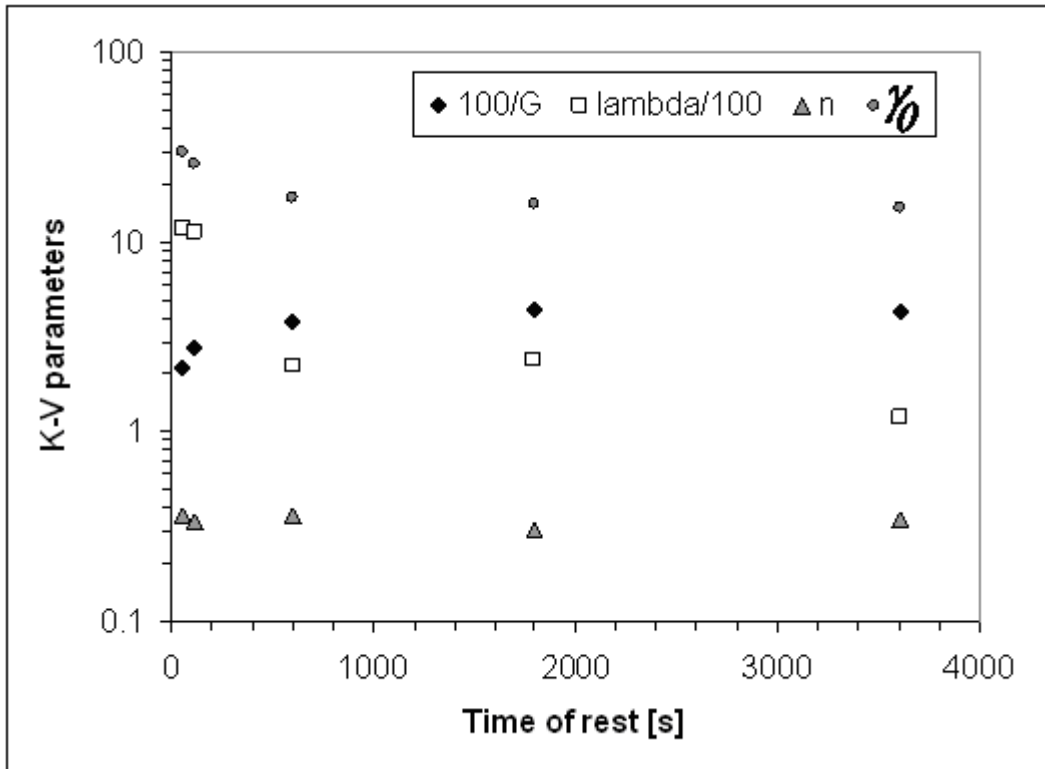
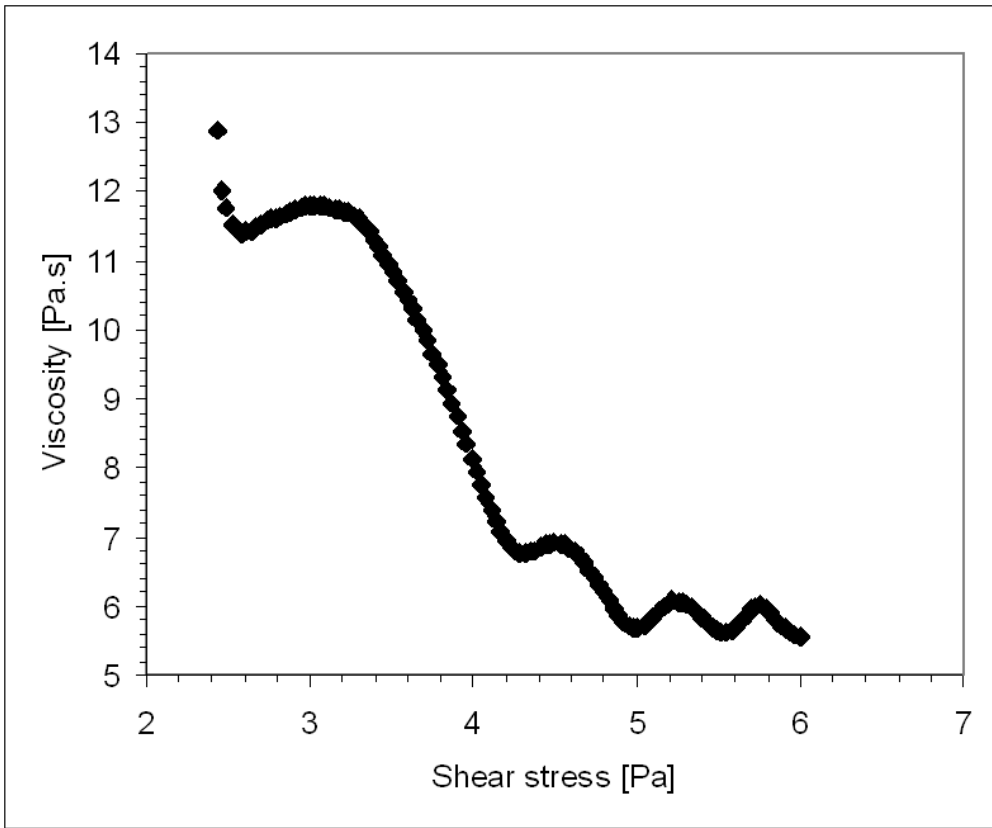


Figure 4: Evolution of the Kelvin-Voigt model parameters as a function of the time of rest.

291
292
293
294
295
296
297

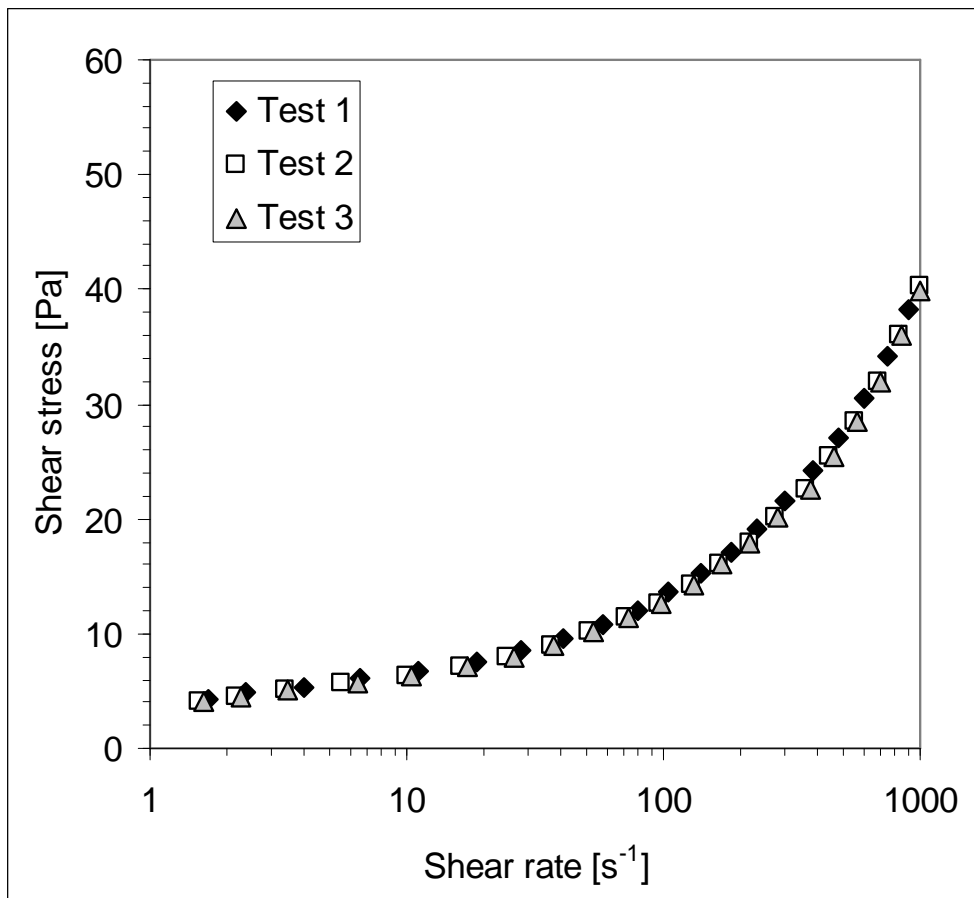


298

299

300

Figure 5: stress-viscosity variations highlighted oscillations with the 4.9% digested sludge.

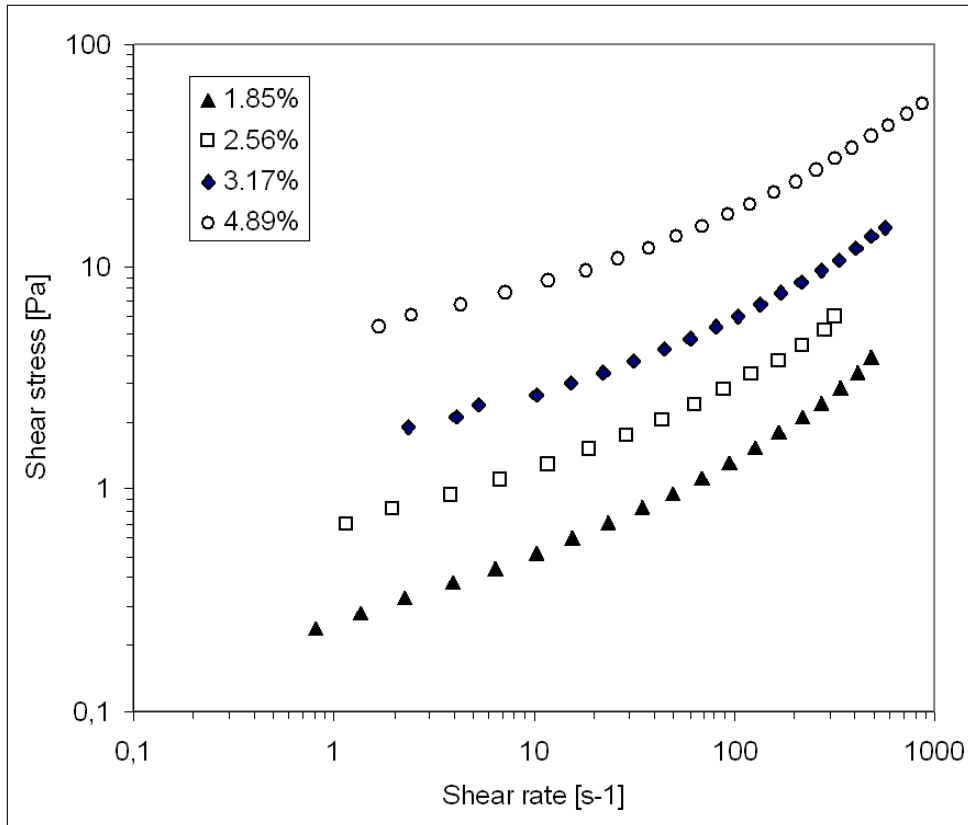


301

302

303

Figure 6: Repeatability of the measurements.



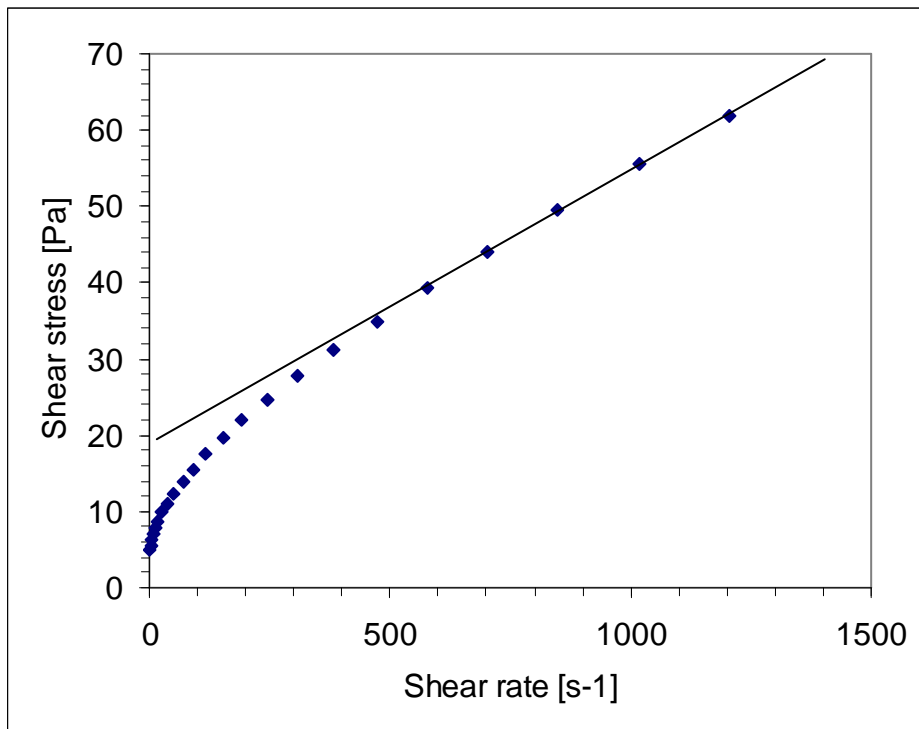
305

306

307

308

Figure 7: Flow curves regarding the concentration of the digested sludge.



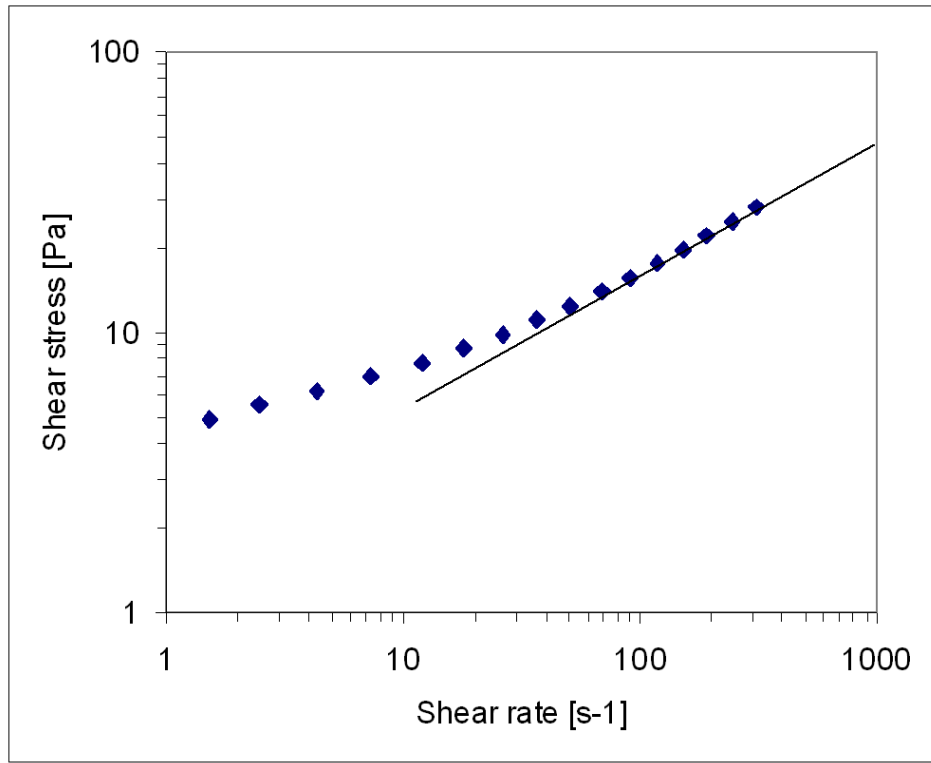
309

310

311

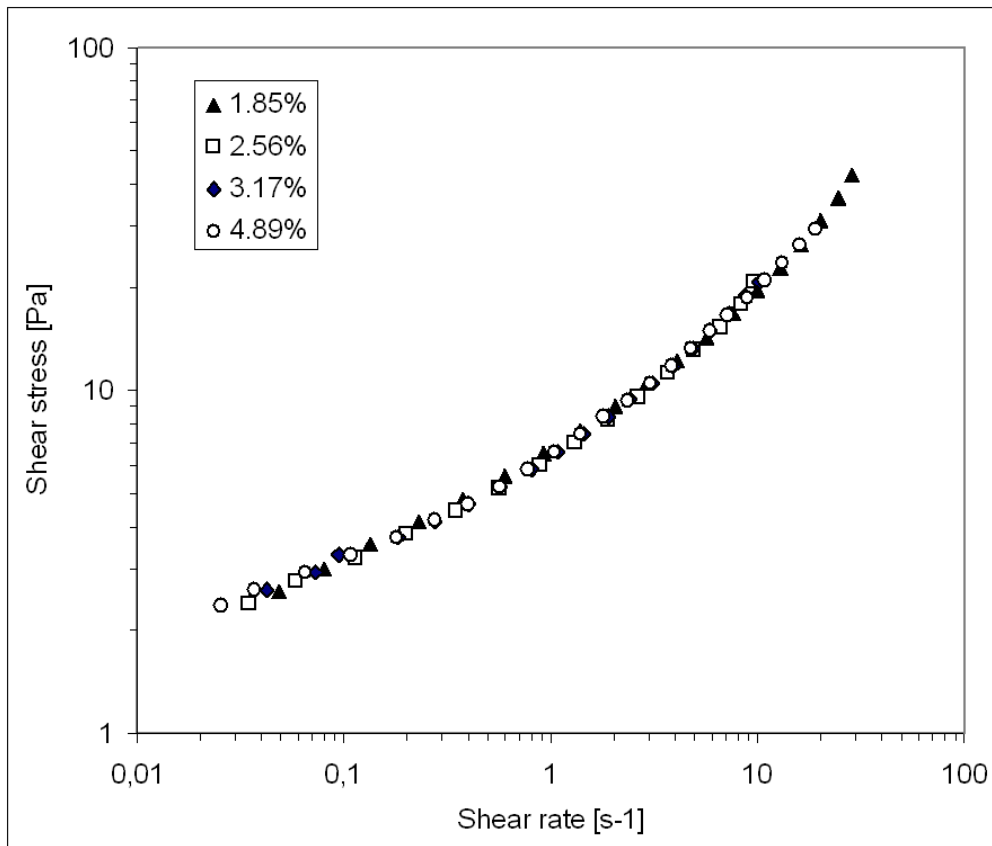
312

Figure 8: At high shear rates, the rheological behaviour can be basically modelled with a Bingham plastic model.



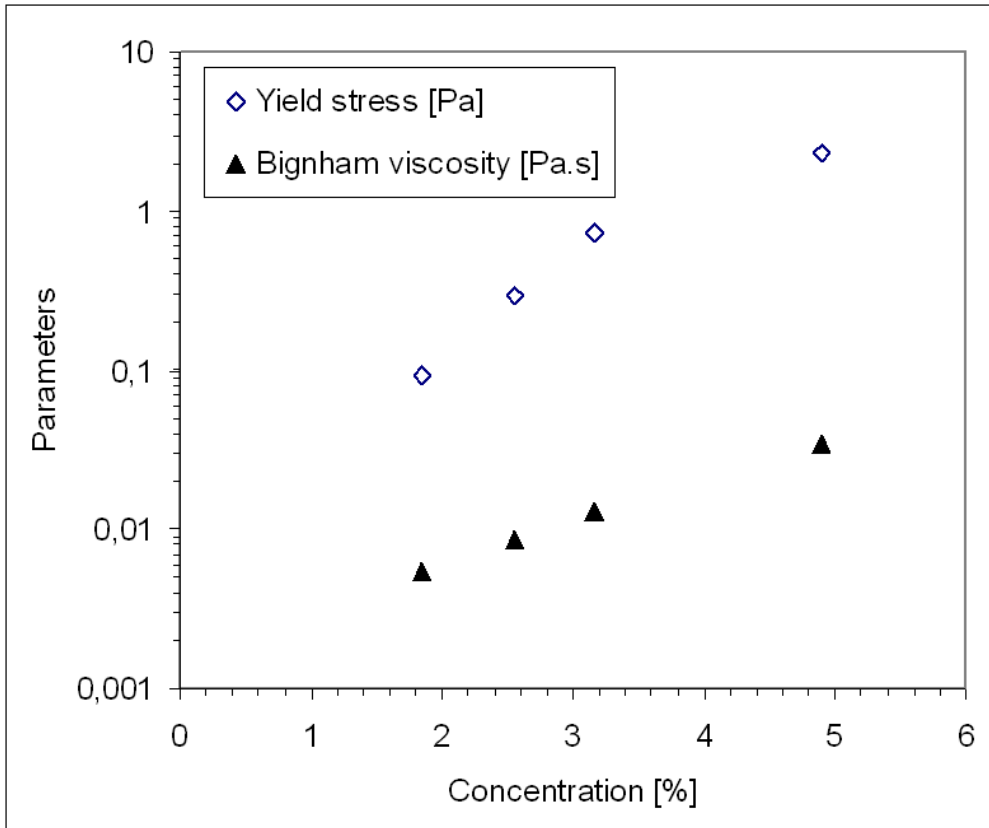
313
314
315
316

Figure 9: At low and intermediate shear rates, the Herschel-Bulkley model or power-law model are the most suitable. The dashed line represents the power-law model $\tau = 2.05 \cdot \dot{\gamma}^{0.45}$.



317
318
319

Figure 10: Dimensionless flow curves of the digested sludge at different concentrations.



320

321 Figure 11: Evolution of the yield stress and the Bingham viscosity regarding the concentration. The

322 parameters of the equations (7) and (8) are respectively $a=0.19 Pa$, $\phi_0=1.17\%$, $m=1.89$ and

323 $\mu_0=0.0018 Pa.s$, $\beta=0.604$.

324

325

326